AMERICAN SOCIETY FOR MICROBIOLOGY | Journal of Virology®

VACCINES AND ANTIVIRAL AGENTS

Surfactin Inhibits Membrane Fusion during Invasion of Epithelial Cells by Enveloped Viruses

Lvfeng Yuan,[a] Shuai Zhang,[a] Yongheng Wang,[a] Yuchen Li,[a] Xiaoqing Wang,[a] Qian Yang[a]

[a]MOE Joint International Research Laboratory of Animal Health and Food Safety, College of Veterinary Medicine, Nanjing Agricultural University. Nanjing, Jiangsu, People's Republic of China

ABSTRACT Because membrane fusion is a crucial step in the process by which enveloped viruses invade host cells, membrane fusion inhibitors can be effective drugs against enveloped viruses. We found that surfactin from *Bacillus subtilis* can suppress the proliferation of porcine epidemic diarrhea virus (PEDV) and transmissible gastroenteritis virus (TGEV) in epithelial cells at a relatively low concentration range (15 to 50 μg/ml), without cytotoxicity or viral membrane disruption. Membrane fusion inhibition experiments demonstrate that surfactin treatment significantly reduces the rate at which the virus fuses to the cell membrane. Thermodynamic experiments show that the incorporation of small amounts of surfactin hinders the formation of negative curvature by lamellar-phase lipids, suggesting that surfactin acts a membrane fusion inhibitor. A fluorescent lipopeptide similar to surfactin was synthesized, and its ability to insert into the viral membrane was confirmed by spectroscopy. *In vivo* experiments have shown that oral administration of surfactin to piglets protects against PEDV infection. In conclusion, our study indicates that surfactin is a membrane fusion inhibitor with activity against enveloped viruses. As the first reported naturally occurring wedge lipid membrane fusion inhibitor, surfactin is likely to be a prototype for the development of a broad range of novel antiviral drugs.

IMPORTANCE Membrane fusion inhibitors are a rapidly emerging class of antiviral drugs that inhibit the infection process of enveloped viruses. They can be classified, on the basis of the viral components targeted, as fusion protein targeting or membrane lipid targeting. Lipid-targeting membrane fusion inhibitors have a broader antiviral spectrum and are less likely to select for drug-resistant mutations. Here we show that surfactin is a membrane fusion inhibitor and has a strong antiviral effect. The insertion of surfactin into the viral envelope lipids reduces the probability of viral fusion. We also demonstrate that oral administration of surfactin protects piglets from PEDV infection. Surfactin is the first naturally occurring wedge lipid membrane fusion inhibitor that has been identified and may be effective against many viruses beyond the scope of this study. Understanding its mechanism of action provides a foundation for the development of novel antiviral agents.

KEYWORDS surfactin, enveloped virus, membrane fusion, fusion inhibitor

In recent years, infectious diseases caused by enveloped viruses, such as hepatitis viruses, human immunodeficiency virus, severe acute respiratory syndrome (SARS) coronavirus, and Ebola virus, have become increasingly common (1, 2). Broad-spectrum drugs that are effective against enveloped viruses are urgently needed to combat these threats. In the swine industry, diarrhea caused by porcine epidemic diarrhea virus (PEDV) and swine transmissible gastroenteritis virus (TGEV) has caused serious economic losses worldwide (3–8). Although vaccines are available for PEDV and TGEV, they are not optimal in terms of safety and efficacy, and large-scale infections often occur.

The capsid of an enveloped virion is typically surrounded by a lipid bilayer contain-

Received 8 June 2018 **Accepted** 25 July 2018

Accepted manuscript posted online 1 August 2018

Citation Yuan L, Zhang S, Wang Y, Li Y, Wang X, Yang Q. 2018. Surfactin inhibits membrane fusion during invasion of epithelial cells by enveloped viruses. J Virol 92:e00809-18. https://doi.org/10.1128/JVI.00809-18.

Editor Julie K. Pfeiffer, University of Texas Southwestern Medical Center

Address correspondence to Qian Yang, zxbyq@njau.edu.cn.

ing embedded proteins. In order to infect a cell, an enveloped virus must fuse its envelope with the cellular membrane so that the envelope chamber is connected to the cytoplasm. The viral genome is then released into the cell, which is a prerequisite for viral replication (9). This process can occur on the plasma membrane or in endosomes, depending on the viral envelope glycoproteins (10). The membrane fusion process is coupled with topological changes in the envelope lipids. From the energy point of view, the outer leaflet of the viral membrane possesses a dramatically unstable positive curvature, due to the small spherical shape of the virus (11). Formation of the lipid stem, the key structure of the membrane fusion intermediate, requires that the outer leaflet of the viral envelope change from a positive to a negative curvature (12). The energy required for this transformation is provided by the refolding of viral fusion protein (13). Some antiviral drugs target membrane fusion proteins and inhibit membrane fusion by blocking allosteric changes in membrane fusion proteins. However, due to the diversity of membrane fusion proteins among viruses and the ability of viruses to mutate rapidly, these drugs have a narrow spectrum and can easily select for drug-resistant strains (14). Fusion inhibitors that target membrane lipids may offer an alternative. To be effective, they require a wedge-shaped amphiphilic structure with a relatively large hydrophilic head and a relatively small hydrophobic tail. The insertion of wedge lipids into the outer leaflet of the envelope stabilizes the positive curvature and reduces the possibility of membrane fusion. Drugs with these properties should be broad-spectrum antivirals, with low cytotoxicity and with reduced ability to select for resistance. Only one class of chemically synthesized compounds has been reported thus far to behave as a lipid-targeted membrane fusion inhibitor (15–17). However, the molecular mechanism underlying their antiviral activity is controversial (18). It is therefore desirable to identify new wedge lipid membrane fusion inhibitors.

Surfactin, which was originally found in *Bacillus subtilis*, is a natural compound with a wide range of biological activities (19). OKB105, a derivative of the well-known *B. subtilis* test strain 168, produces high levels of surfactin (20). The inhibitory activity of surfactin against multiple enveloped viruses has been reported (21, 22), as well as its anti-TGEV effect (23). However, the specific mechanism remains to be elucidated. Surfactin is a cyclic molecule consisting of a heptapeptide and a fatty acid, and it has a structure that is consistent with the characteristics of a wedge lipid: two acidic amino acid residues form a relatively large hydrophilic head, while the long-chain fatty acid forms a relatively small hydrophobic tail (24), as shown in Fig. 1A. We therefore predicted that surfactin would exhibit the ability to inhibit viral membrane fusion. Here we confirm that surfactin is a membrane fusion inhibitor and that this property accounts for its antiviral activity. These results provide a theoretical basis for the development of new drugs active against enveloped viruses.

RESULTS

Surfactin from *B. subtilis* inhibits PEDV and TGEV infectivity. Surfactin was purified from the medium of a *B. subtilis* OKB105 culture and was identified by high-performance liquid chromatography (HPLC) coupled with mass spectrometry (MS). By comparison to the surfactin standard, which is 98% pure, almost all of the peaks correspond to the various homologues of surfactin (Fig. 1B). Peaks with differing *m/z* values are due to the diversity of the fat chain or the presence of one or more isotopes in the same molecule (Fig. 1C and D). The molecular weights of the surfactin homologues in the purified product are consistent with those of the standard, but the proportion of surfactin homologues is different (Fig. 1B). The concentration of surfactin in the purified product was obtained by comparing the integrated peak area with the surfactin standard and was estimated to be 87%.

To investigate the cytotoxicity of surfactin, we evaluated its ability to cause hemolysis of red blood cells (RBC) and to affect the viability of IPEC-J2 and Vero cells over a range of concentrations. Lysophosphatidylcholine (LPC) has strong hemolytic activity and was used as a positive control. Dielaidoylphosphatidylethanolamine (DEPE), one of the normal components of the cell membrane, was used as a negative control. This

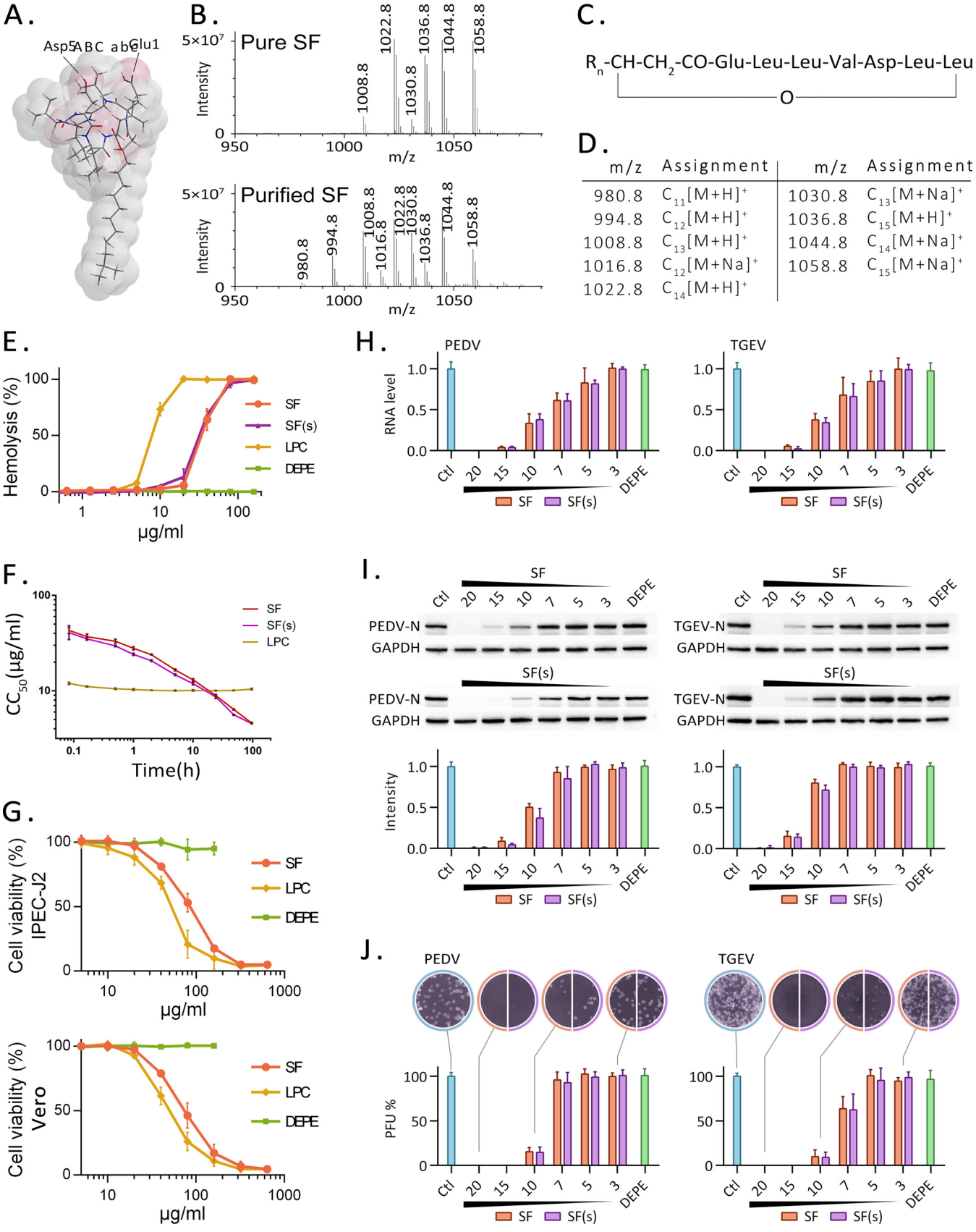

FIG 1 Surfactin and its antiviral activity. (A) Three-dimensional structure of surfactin, drawn with Chem3D, according to reference 46. (B) Mass spectra for the surfactin (SF) standard (98% purity) and for surfactin purified from *B. subtilis* OKB105. (C) General structural formula for surfactin homologues (46). (D)

(Continued on next page)

compound differs from LPC in that it has two fatty acid chains and no hemolytic activity. Hemolytic activity increased as the surfactin concentration increased (Fig. 1E). Hemolysis was barely detectable at 20 μg/ml but reached nearly 100% at 4 times that concentration. The time course of hemolytic activity was also measured. The concentrations of surfactin purified from *B. subtilis* OKB105 (SF) and the surfactin standard [SF(s)] were plotted against the time required to achieve 50% hemolysis (Fig. 1F). The purified surfactin sample and the surfactin standard have almost identical half-hemolytic concentration curves. For LPC, which has a steep dose response and strong hemolytic activity, half-hemolysis occurs at 10 μg/ml in 10 min, but no further hemolysis occurs during the next 96 h. Surfactin at levels higher than 20 μg/ml decreases the viability of IPEC-J2 cells and Vero cells (Fig. 1G) and is similar to LPC, the positive control.

The antiviral activity of surfactin was assayed using PEDV- and TGEV-infected cells. Virus-infected cells were cultured in media containing different concentrations of purified surfactin or the surfactin standard. Twelve hours after infection, viral RNA replication and protein production levels were measured (Fig. 1H and I), and the titers of infectious virus particles in the medium were determined (Fig. 1J). Surfactin concentrations above 15 μg/ml almost completely inhibited the replication of either virus. Since surfactin concentrations at this level cause no detectable cytotoxicity, this result suggests that a potent antiviral effect can be obtained at 15 to 20 μg/ml without harming cells. Because the purified surfactin sample prepared in this study and the surfactin standard have similar cytotoxicities and antiviral activities, subsequent studies were conducted using our purified surfactin. Since both PEDV and TGEV are coronaviruses, with similar susceptibilities to surfactin, we hypothesized that surfactin has similar mechanisms of action on PEDV and TGEV, and subsequent experiments were conducted on TGEV.

Surfactin acts directly on viruses. In order to determine the stage at which surfactin exerts its anti-TGEV effect, surfactin, DEPE, or neutralizing antibodies were added to the virus or cells at different times before or during infection (Fig. 2A). The infection process was divided into preinfection, virus adsorption (at 4°C), virus invasion (the first hour after infection at 37°C), and replication (1 to 12 h postinfection [hpi]) phases (Fig. 2A). Twelve hours after infection, samples were harvested and were analyzed to determine the titers of infectious particles in the culture medium (Fig. 2B) and to measure the levels of viral RNA (Fig. 2C) and viral protein (Fig. 2D and E). The negative control DEPE had no significant effect at any stage. In contrast, surfactin and neutralizing antibodies completely inhibited TGEV production if applied throughout the experiment (group 2) or if applied to the virus prior to and during adsorption (group 5). Both reagents also completely eliminated infectious TGEV in the culture medium if applied during the replication stage (group 8), although neither reagent affected levels of viral nucleic acid or protein. These results suggest that surfactin is similar to TGEV neutralizing antibody, which acts directly on TGEV particles and causes them to lose their infectivity. The dramatic difference between groups 5 and 6 indicates that surfactin and antibody have little or no effect during the adsorption phase. Surfactin treatment of cells prior to TGEV invasion (groups 3 and 4) also reduced the production of viral RNA, protein, and infectious particles, although the effect was far greater when the virus was pretreated (group 5). It is worth mentioning that the following experimental results can also provide evidence for the direct action of surfactin on TGEV.

FIG 1 Legend (Continued)

Assignment of the surfactin homologues. The subscript indicates the number of carbon atoms in the aliphatic chain. (E) Hemolytic curves generated by surfactin, LPC, and DEPE. One hundred percent is defined as the hemolysis generated by treatment of red blood cells with 0.1% Triton X-100. (F) Time course for half-hemolytic activity. Shown are the concentrations of purified surfactin (SF), the surfactin standard [SF(s)], and LPC, as well as the incubation times required for 50% hemolysis. CC_{50}, 50% cytotoxic concentration. (G) Cytotoxicity of SF, LPC, or DEPE on IPEC-J2 cells or Vero cells, measured by the MTT method after 12 h of incubation. Due to the solubility problem, DEPE concentrations above 200 μg/ml cannot be tested. (H to J) Cells were infected with PEDV or TGEV for 12 h in the presence or absence (Ctl) of surfactin. Surfactin concentrations (in micrograms per milliliter) are given below the graphs and above the Western blots. After the samples were harvested, the virus genome was detected by qRT-PCR (H), the virus protein was detected by Western blotting (I), and the infectious particles in the culture medium were detected by plaque formation (J). N, nucleoprotein.

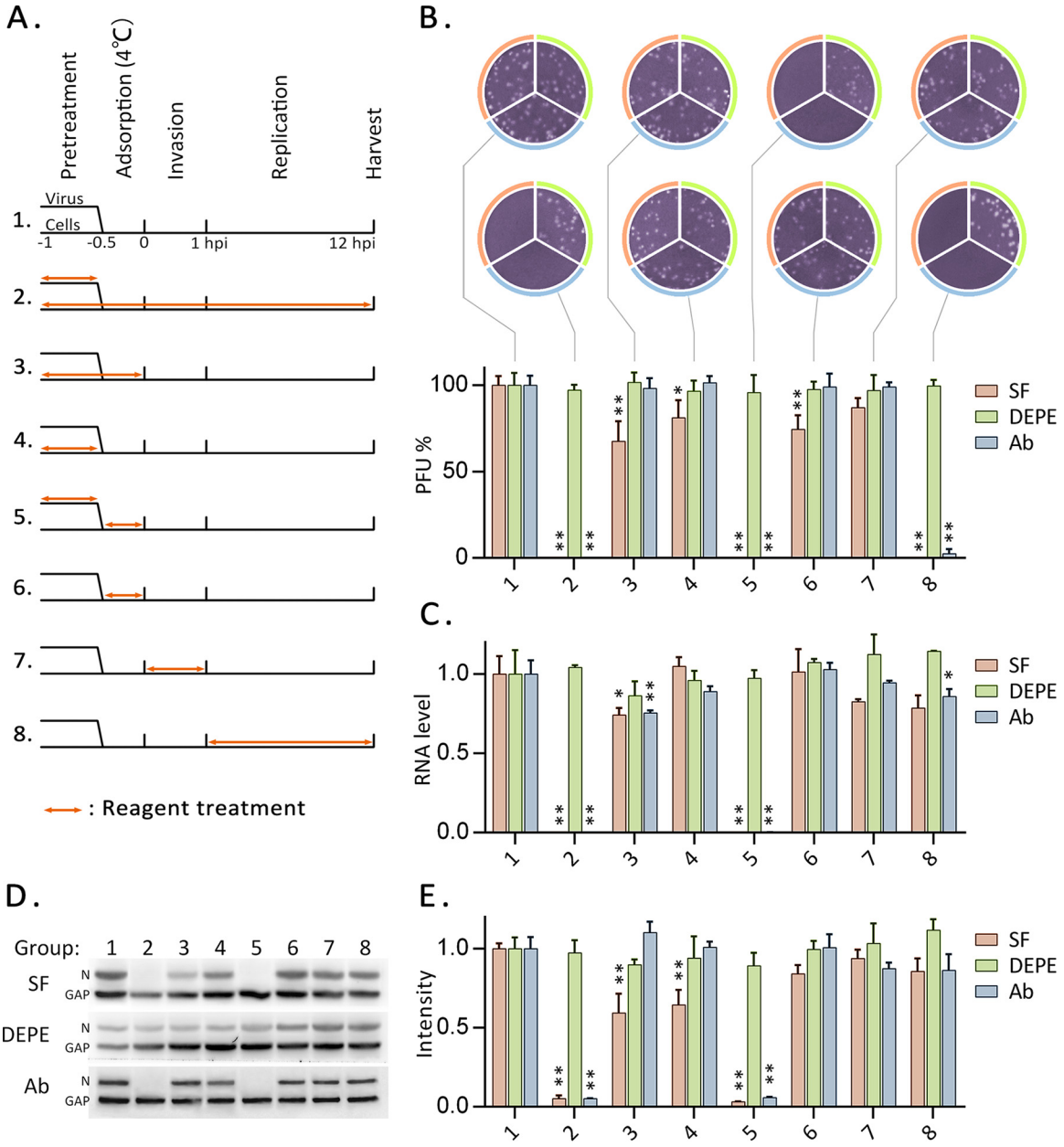

FIG 2 Time-of-addition experiments. (A) IPEC-J2 cells or TGEV was treated with surfactin, DEPE, or antibodies at different times before and after infection. Double-headed orange arrows indicate the presence of the reagent. The experiments are identified in the text by the numbers on the left. Samples were harvested at 12 hpi. (B) Infectious particles in the culture medium were detected by plaque formation. The histogram summarizes the plaque assay results. Numbers below the graph correspond to the numbering of experiments in panel A. (C) Copies of the RNA genome of TGEV were quantitated by qRT-PCR. (D) The nucleoprotein of TGEV was detected by Western blotting. (E) Histogram of the Western blot results showing band intensities. Each experiment was repeated three times. Values were normalized against those for group 1 (no treatment) and are plotted as means ± standard deviations. Significance (*, $P < 0.05$; **, $P < 0.01$) was calculated for each reagent versus group 1 by use of a two-tailed *t* test.

Surfactin acts on viral lipids. The lipid bilayer of the viral envelope is obtained from the host cell and is rigid at 4°C (25). A rigid membrane is less likely to accept membrane-intercalating agents (26). To test whether interaction with lipids is required for virus inactivation, TGEV was exposed to various concentrations of antiviral agents at 4°C or 37°C and was then assayed for its ability to infect cells in a plaque assay. Neutralizing antibody was able to bind to the viral glycoprotein at either 37°C or 4°C and to block infection. However, about 4-fold more antibody was required at 4°C than at 37°C to achieve the same antiviral effect (Fig. 3A, bottom). The membrane fusion

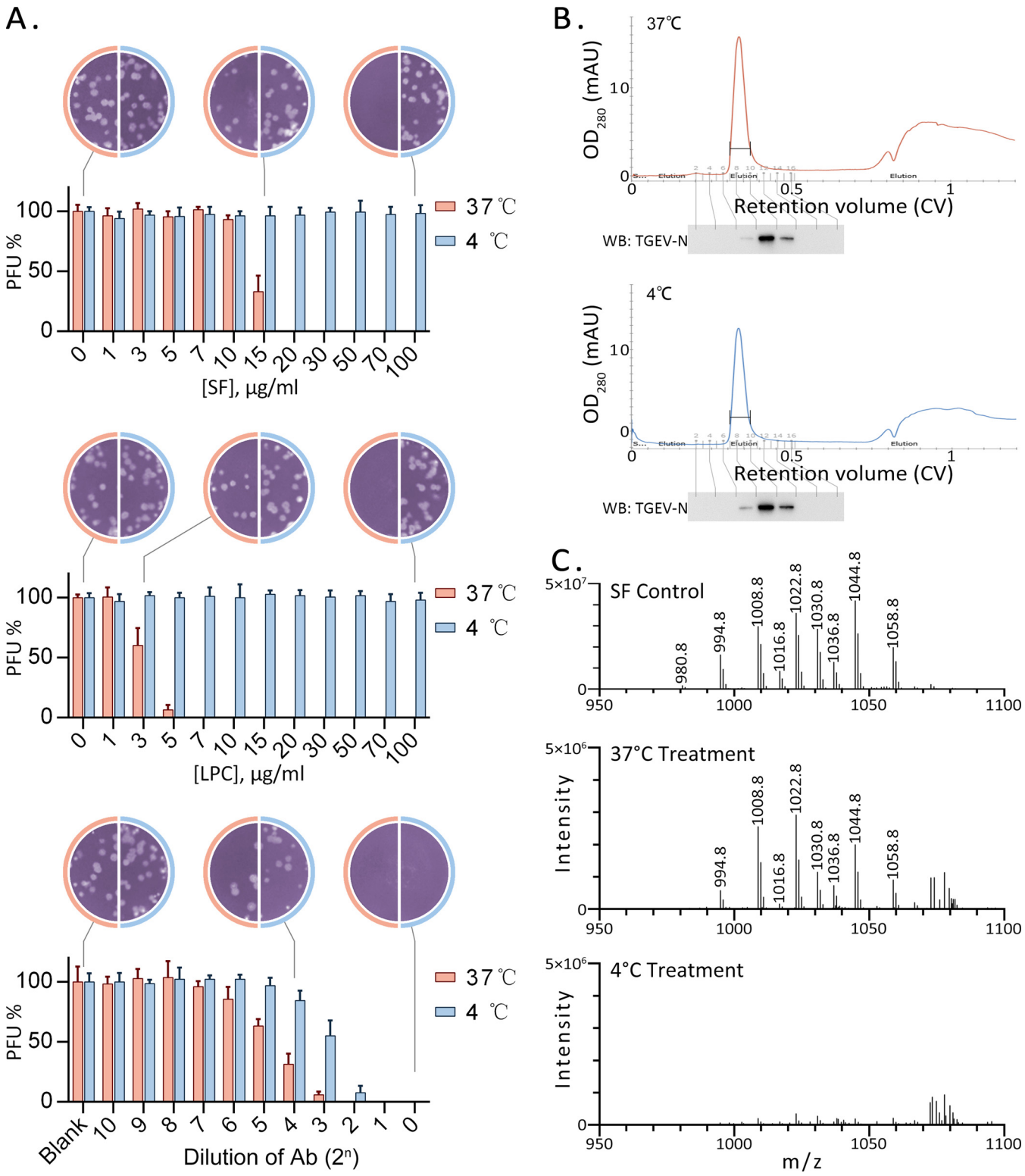

FIG 3 Surfactin acts on viral lipids. (A) TGEV was incubated with different concentrations of surfactin, LPC, or an antibody (Ab), at 37°C or 4°C, for 10 min. Samples were diluted 50-fold, and residual infectious particles were then detected by a plaque assay. Each histogram represents results from three independent experiments. Plaque counts from the untreated sample were defined as 100%. (B) Gel filtration chromatography of TGEV treated with surfactin at 37°C or 4°C. Surplus surfactin was removed, and the virus-containing eluate was collected at a retention of about 0.35 column volume (CV). The presence of TGEV was further confirmed by Western blotting (WB). mAU, milli-absorbance unit. (C) The surfactin remaining in the viral particles was extracted and analyzed by LC-MS, along with the purified surfactin (SF Control) used in this experiment. Surfactin can be detected at low levels in virus incubated at 37°C. In contrast, at the same sensitivity, it is barely detectable in virus incubated at 4°C.

inhibitor LPC, which is known to be inserted into the viral envelope (27), had almost no antiviral activity at 4°C (Fig. 3A, center). Surfactin showed a similar trend (Fig. 3A, top). This result suggests that the antiviral effect of surfactin is not associated with viral proteins and is more likely to be associated with viral envelope lipids.

To clarify whether surfactin is inserted into the viral envelope, TGEV was treated with surfactin at 4°C or 37°C, and excess surfactin was removed using gel filtration at a low temperature. Pure TGEV was eluted with a retention of 0.35 column volume, and fractions containing virus were collected (Fig. 3B). Surfactin could be extracted and detected in the sample treated at 37°C but was barely detectable in the sample treated at 4°C (Fig. 3C). This result supports the hypothesis that surfactin is inserted into the envelope membrane.

To further corroborate the insertion of surfactin into the envelope, two synthetic lipopeptides (SysLP1 and SysLP2) based on the structure of surfactin were designed and synthesized (Fig. 4A; cf. Fig. 1A). The only difference between SysLP1 and SysLP2 is the biphenylene in the fatty acid moiety of the latter (Fig. 4A). The synthetic lipopeptides exhibit nearly identical antiviral activities and are similar to surfactin (Fig. 4B). Because the biphenyl and amide groups in the synthetic molecules are conjugated and may have optical activity, dual-wavelength fluorescence scanning was conducted to evaluate their fluorescence. SysLP1 had no fluorescence activity in the UV and visible ranges, while SysLP2 had a significant peak of fluorescence (Fig. 4C), with maximum excitation at 280 nm and maximum emission at 370 nm. The fluorescent behavior of the hydrophobic moiety of an amphiphilic molecule is affected by the microenvironment. The spectral changes can be used to indicate whether the molecule is inserted into a membrane (26). Here, *n*-hexane was used as a solvent to simulate a hydrophobic environment. SysLP2 dissolved in *n*-hexane and SysLP2 inserted into a lipid membrane would be in similar hydrophobic environments. After SysLP2 was dissolved in *n*-hexane, the fluorescence emission wavelength shifted to 346 nm (Fig. 4D). When SysLP2 was added to TGEV in phosphate-buffered saline (PBS), the maximum emission was at 346 nm, identical to that in *n*-hexane (Fig. 4D). This result further demonstrates that SysLP2 has the ability to insert into the viral envelope, suggesting that surfactin has the same property.

Surfactin inactivates TGEV without envelope disruption. Because some direct-acting antivirals disturb the envelope structure, they may also damage the cell membrane at similar concentrations, making their use hazardous (28). Mature mammalian red blood cells have no nucleus and low cell membrane repair ability. In an earlier test, 20 μg/ml of surfactin did not cause RBC content leakage for as long as 3 h (Fig. 1F). This indicates that surfactin has little effect on cell membrane integrity at this concentration. We therefore investigated the effect of surfactin on envelope integrity. Purified TGEV was treated with surfactin, LPC, Triton X-100, or a solvent. The samples were centrifuged through a linear 20%-to-50% sucrose gradient, and each gradient was collected in 26 fractions (Fig. 5A). The fraction density from bottom to top differed linearly, and the density curves for the four samples were well matched (Fig. 5B). Viral proteins in each fraction were detected by Western blotting (Fig. 5C). Spike protein is present in the viral envelope, and the nucleoprotein forms the capsid with the viral genome. As shown in the control sample, intact TGEV was found in fractions containing approximately 34% sucrose, where the spike protein and nucleoprotein were both present. When TGEV was treated with Triton X-100, about half of the TGEV particles separated into nucleocapsid and envelope membrane components. The virus capsid was found in the fraction containing 46% sucrose, while the envelope debris remained in the sample layer. For samples treated with either surfactin or LPC, no envelope leakage was observed. The results obtained using quantitative real-time PCR (qRT-PCR) were similar (Fig. 5D). Only Triton X-100 treatment affected viral integrity. The titers of infectious virus particles in the sample were determined using plaque assays (Fig. 5E). Interestingly, although surfactin and LPC do not appear to affect virus integrity, both treatments abolish infectivity.

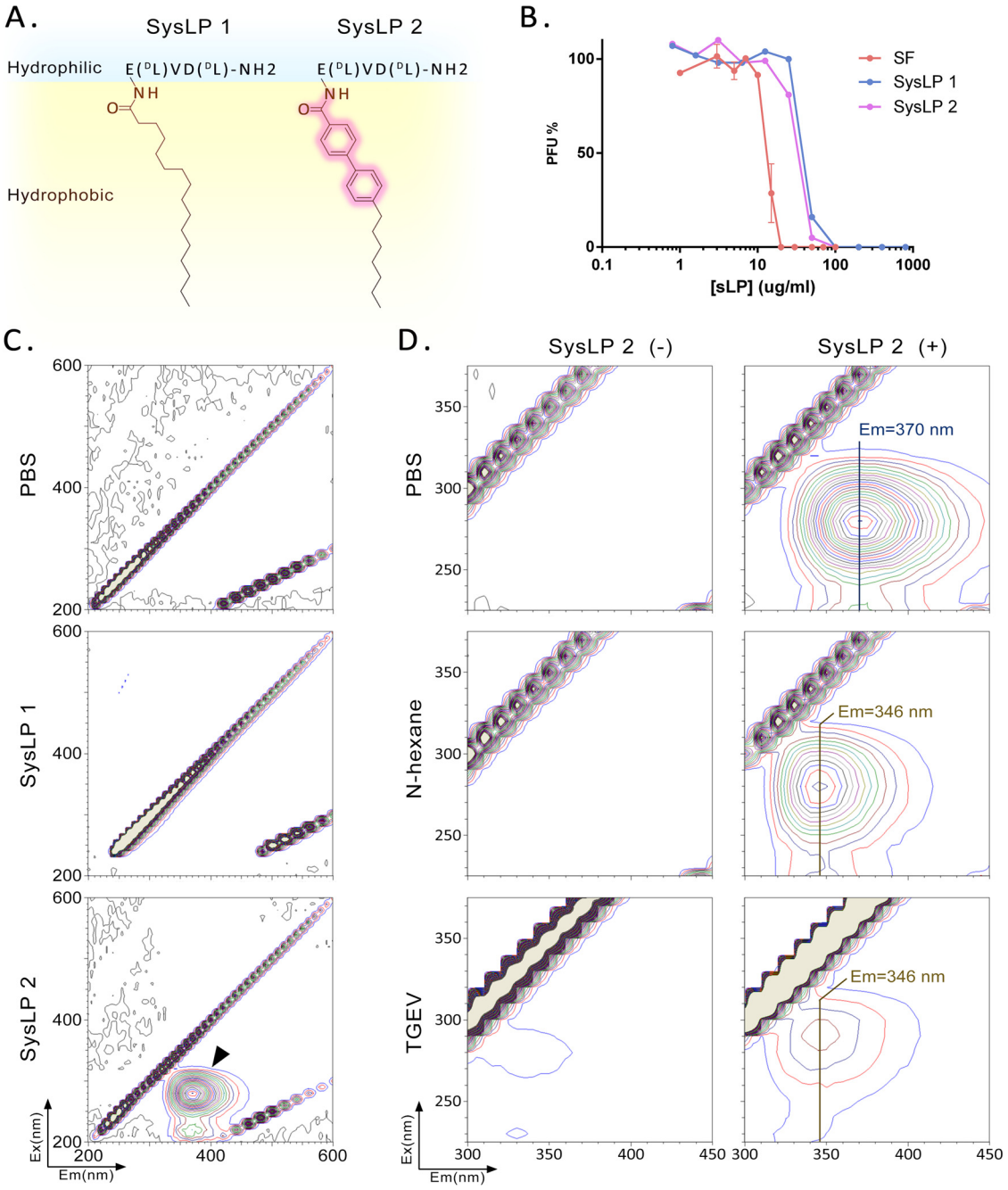

FIG 4 Insertion of fluorescent lipopeptides into viral membranes. (A) Molecular formulas for the two synthetic lipopeptides used in this experiment. (B) Antiviral activities (using TGEV) of synthetic lipopeptides (sLP) and surfactin, measured in a plaque assay. (C) Dual-wavelength fluorescence scans of solutions of synthetic lipopeptides. A solvent (PBS) and SysLP1 showed no fluorescence at UV and visible wavelengths. SysLP2 fluoresced at an excitation wavelength of 280 nm and an emission wavelength of 370 nm, as indicated by the arrows. (D) Dual-wavelength fluorescence scans of SysLP2 in different samples. The emission wavelength is 370 nm in PBS, as opposed to 346 nm in *n*-hexane or in PBS containing TGEV.

Observation of differently treated TGEV by electron microscopy provides more support for the effect of surfactin on envelope structure (Fig. 5F). Surfactin and LPC treatments do not alter the capsule shape or spike protein arrangement and produce the same effects as the control treatment. In contrast, it is difficult to find a complete virus particle in samples treated with Triton X-100. Instead, polygonal particles with a diameter of about 70 nm can be observed. We speculate that these particles are virus capsids.

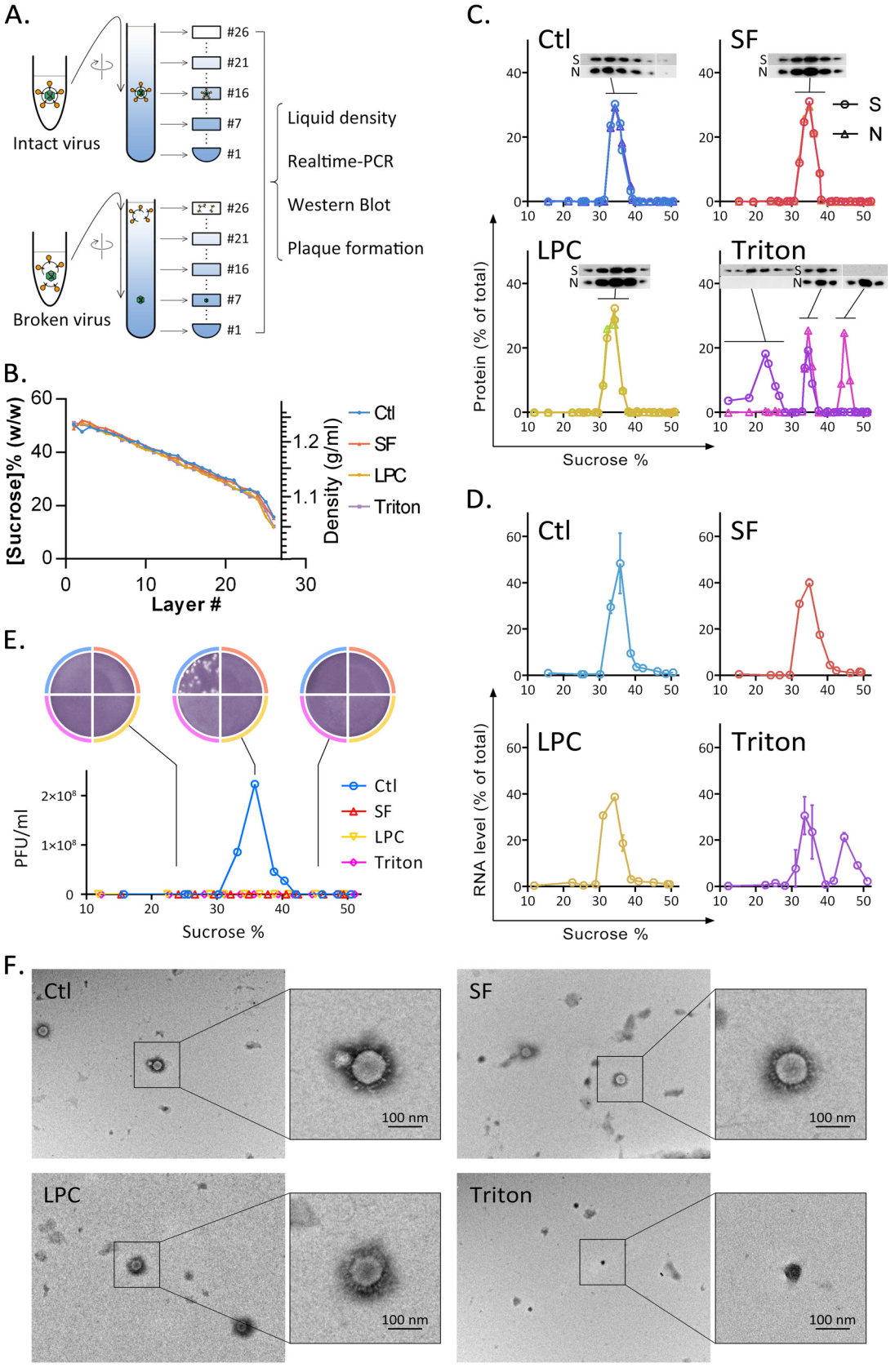

FIG 5 Surfactin-treated TGEV retains envelope integrity. (A) TGEV was incubated with different reagents at 37°C for 30 min. Mixtures were sedimented through a linear sucrose density gradient, and 26 fractions were collected after ultracentrifugation. Several methods were used to analyze the viral components in each fraction. (B) The sucrose content (expressed as a percentage)

(Continued on next page)

Surfactin inhibits the fusion between viral and cellular membranes. Since surfactin affects viral lipid components but not viral integrity, we investigated whether surfactin interferes with viral adsorption or membrane fusion. In these experiments, TGEV was treated with different reagents and was adsorbed to cells; then unbound viruses were washed away, and cells were harvested. qRT-PCR analysis showed that treatments with surfactin and LPC did not affect the adsorption of virus, whereas neutralizing antibodies significantly reduced viral adsorption (Fig. 6A). Since surfactin does not inhibit viral replication (Fig. 2), it seems most likely that the antiviral effects occur during membrane fusion in the invasion stage.

To test whether surfactin inhibits fusion between the viral envelope and the cell membrane, we took advantage of the self-quenching properties of octadecyl rhodamine (R18). TGEV was labeled with self-quenching concentrations of octadecyl rhodamine (R18) and was then incubated with cells at 4°C for 30 min to allow binding without triggering fusion. The pH was then adjusted to 5 and the temperature raised to 37°C to permit the virus to fuse with the cell membrane. The membrane fusion process dequenches R18 (Fig. 6B) and can be observed in cell samples by use of fluorescence microscopy (Fig. 6C). In a kinetic experiment, fluorescence intensity was continuously monitored every 30 s, for 1 h. As shown in Fig. 6D, the virus in the control sample fused to target cells, and fluorescence gradually increased to 30% (relative to the fluorescence intensity after the addition of Triton X-100, which was defined as 100%), in 1 h. The slope of the curve decreased with time and was predicted to reach a maximum value of 38.77%. DEPE, a cylindrically shaped lipid, does not affect membrane fusion and generates a curve similar to that for the control. In contrast, LPC and surfactin both behave as effective membrane fusion inhibitors.

Surfactin insertion increases the positive curvature of the lipid monolayer. Stalk formation, the first step of membrane fusion, requires energy to generate a negatively curved surface that couples the outer layer of the envelope and the cell membrane. The insertion of surfactin into the virus envelope may make viral membrane fusion energetically unfavorable (26). We therefore tested whether surfactin inhibits the development of negative curvature. Lipid membrane samples were prepared by mixing DEPE with surfactin, LPC, or cholesterol at different ratios. For each mixture, the temperature at which the lamellar liquid-crystalline (L_α) phase transitioned to the inverted-hexagonal (H_{II}) phase (designated T_H) was observed by differential scanning calorimetry (DSC) (Fig. 7A). The experiment exploits the facts that lipid molecules in the L_α phase are in a planar membrane and the hydrophilic groups occupy the same area as the hydrophobic groups. However, lipid molecules in the H_{II} phase are in a planar or negatively curved lipid membrane, and the area occupied by the hydrophilic groups is equal to or less than the area of the hydrophobic groups. In a membrane composed of columnar lipid DEPE, the incorporation of a small amount of a cone-shaped lipid, such as cholesterol, will contribute to the formation of negative curvature. This favors the H_{II} phase and results in a lower phase transition temperature. Conversely, the incorporation of inverted-cone-shaped lipids is not conducive to the formation of negative curvature and therefore increases the phase transition temperature. The DSC results are shown in Fig. 7B. The DSC curve for each lipid mixture was fitted to a Gaussian function, and the T_H value was calculated. The T_H values plotted against the percentages of lipid incorporation are shown in Fig. 7C. By use of estimates from linear regression, a 1% increment in the cholesterol concentration will decrease the phase transition temperature by 0.76 $\pm$ 0.02°C (Fig. 7C), in agreement with a previous study (29). In contrast,

FIG 5 Legend (Continued)
was calculated from the density of each fraction. (C) Viral proteins in each fraction were detected using Western blotting. S, spike protein from the viral envelope; N, nucleoprotein from the viral capsid. The *x* axis in each profile shows the sucrose content (expressed as a percentage) in each fraction. (D) Fractions were analyzed for the presence of viral RNA using qRT-PCR. One hundred percent is defined as the total amount of RNA detected in the corresponding experiment. (E) Infectious particles were detected using a plaque assay. Infectious virus was detected only in fraction 16 and adjacent fractions for the untreated TGEV sample. (F) Virus structure visualized using transmission electron microscopy. Virus particles in the surfactin- and LPC-treated samples were structurally intact, as was also the case for the untreated control. Virus debris was found only in Triton X-100-treated samples.

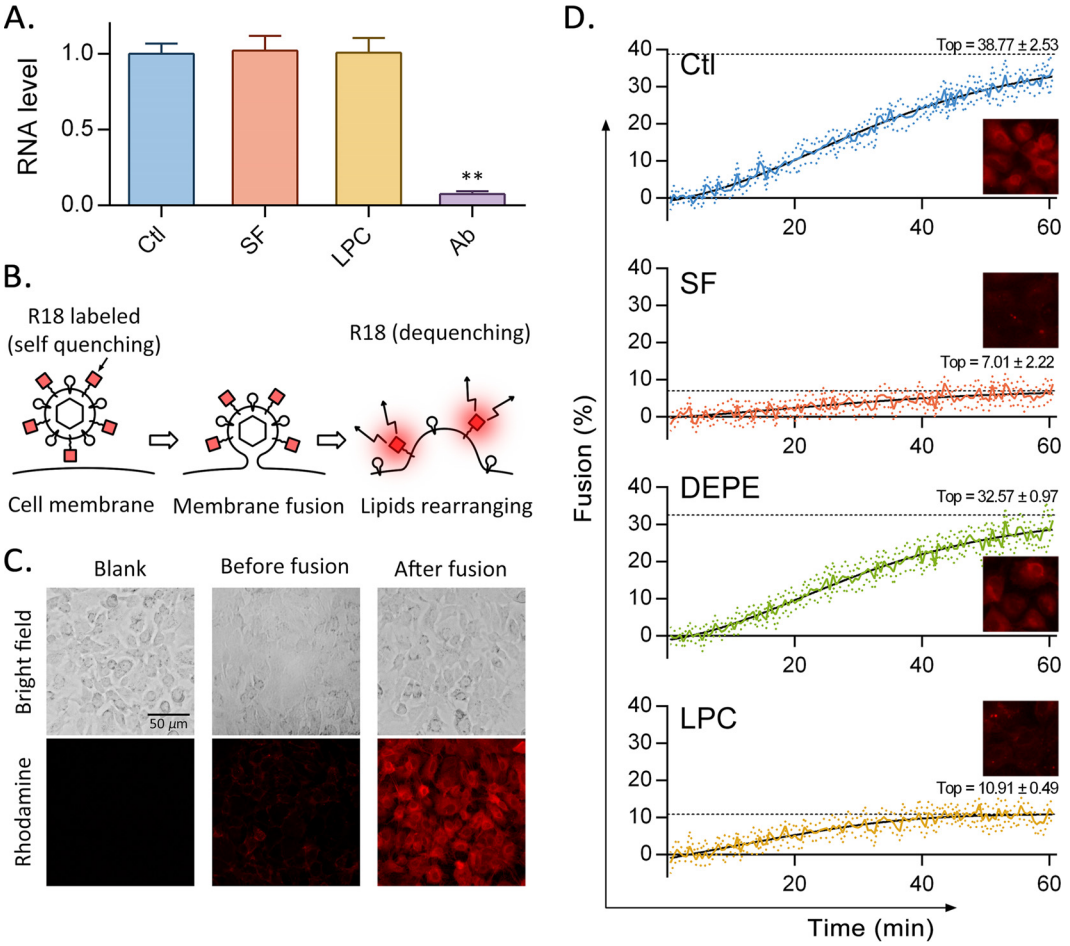

FIG 6 Surfactin inhibits viral membrane fusion. (A) TGEV treated with different reagents was allowed to adsorb to cells. The cells were then washed, and qRT-PCR was used to detect the viral RNA remaining with the cells. (B) Mechanism underlying the membrane fusion inhibition assay. The octadecyl rhodamine (R18) label attached to TGEV is dequenched after the virus fuses with the cellular membrane. (C) After R18-labeled TGEV was added to ST cells, fluorescence was observed before and after incubation for 1 h at 37°C using a fluorescence microscope. (D) R18-labeled TGEV was first exposed to surfactin, DEPE, LPC, or a solvent (Ctl) for 10 min at 37°C and then incubated with ST cells in a 96-well plate at 4°C for 1 h. The virus-cell complexes were washed and then adjusted to pH 5 with HCl. Fluorescence intensity was continuously monitored at 37°C for 1 h. After the kinetic experiment, Triton X-100 was added to each well to maximize membrane fusion, and the resulting fluorescence intensity was defined as 100% fusion. Each plot shows the results of 7 independent experiments (means ± standard deviations, represented by colored lines with colored dots). A sigmoidal curve was fit to the data (solid black lines). The estimated maximum values are shown by dotted black lines.

the phase transition temperature increased by 0.48 ± 0.01°C or 0.38 ± 0.03°C per 1% increment in the surfactin or LPC concentration, respectively (Fig. 7C). These data demonstrate that surfactin, like LPC, disfavors the negative curvature of a membrane monolayer.

Oral administration of surfactin protects piglets from PEDV infection. It has been reported that the oral bioavailability of cyclic peptides with >4 residues is extremely low (30). We hypothesize that orally administered surfactin will remain in the intestinal lumen rather than causing hemolysis after absorption. Surfactin in the intestinal lumen may have an antiviral effect similar to that in *in vitro* experiments. The experiments in this part of our investigation were performed with PEDV. CV777 was used *in vitro*, and tissue extracts from PEDV-infected pigs were used *in vivo*.

In an acute toxicity study, mice were orally administered surfactin in a single dose of 0, 4, 20, 100, or 500 mg/kg of body weight (bw). Death was observed only in the highest-dose group in the first 48 h (Fig. 8A). For subchronic toxicity assessment, mice were orally administered surfactin for 28 days. The daily dose was 0, 4, 20, or 100 mg/kg

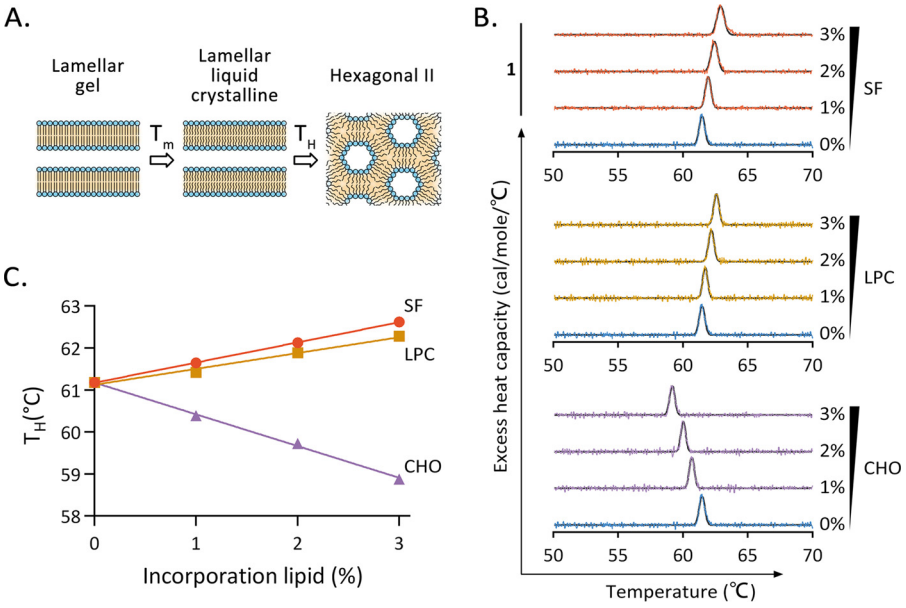

FIG 7 Surfactin increases the positive curvature of the membrane. (A) Mechanism underlying the membrane curvature assay. During the heating process, the planar liquid-crystalline (L_α)-phase dielaidoylphosphatidylethanolamine (DEPE) changes to an inverted-hexagonal (H_{II}) state with abundant negative curvature at the phase transition temperature (T_H). (B) The excess heat capacities of DEPE samples with the indicated lipid compositions were measured by differential scanning calorimetry during heating. CHO, cholesterol. (C) T_H of each sample plotted against the fraction (expressed as a percentage) of lipid incorporated.

bw for each group. During this experiment, no death was observed. The mice in the high-dose group lost weight. The weight gain of the intermediate-dose group was significantly lower than that of the blank group (Fig. 8B). Daily oral surfactin did not affect RBC, white blood cells (WBC), or platelets (PLT) in mice. However, the level of alanine aminotransferase (ALT) in the blood of the high-dose group was significantly increased, indicating the presence of liver damage (Fig. 8C). Mouse jejunal contents were heated and centrifuged to reduce protein composition. After serial dilution, a plaque reduction assay was performed to estimate the anti-PEDV activity (Fig. 8D). The results showed that with an increase in the oral surfactin dose, the anti-PEDV activity of jejunum contents in mice gradually increased (Fig. 8E). Daily oral doses in excess of 20 mg/kg bw will significantly increase the anti-PEDV property of jejunal contents. Therefore, the daily oral dose was set to 20 mg/kg bw.

Next, we explored whether surfactin can protect piglets from PEDV challenge. Newborn pigs were challenged with PEDV at the age of 2 days, and all pigs died within 48 h. In the surfactin treatment group, the piglets were orally administered surfactin every 6 h starting at the age of 1 day, and the daily dose was 20 mg/kg bw. After PEDV challenge, no death was observed within 48 h. All piglets were sacrificed at 48 hpi. Jejunal hyperemia and colonic tympanites could be seen in the PEDV group piglets. In contrast, in the surfactin treatment group, there were no obvious pathological changes in the intestines (Fig. 8F). The histopathological results for the jejuna further confirmed that jejunal hyperemia was observed only in the piglets in the PEDV group (Fig. 8G). Finally, the level of the PEDV genome in jejunal tissue was quantified by qRT-PCR. PEDV was undetectable in the surfactin treatment group, as well as the blank group (Fig. 8H).

DISCUSSION

In this study, surfactin purified from the medium of *Bacillus subtilis* OKB105 was characterized by mass spectrometry. Its composition was identical to that of a surfactin standard, and its molecular masses were consistent with those reported for surfactin homologues (20). We also demonstrate, for the first time, that surfactin possesses

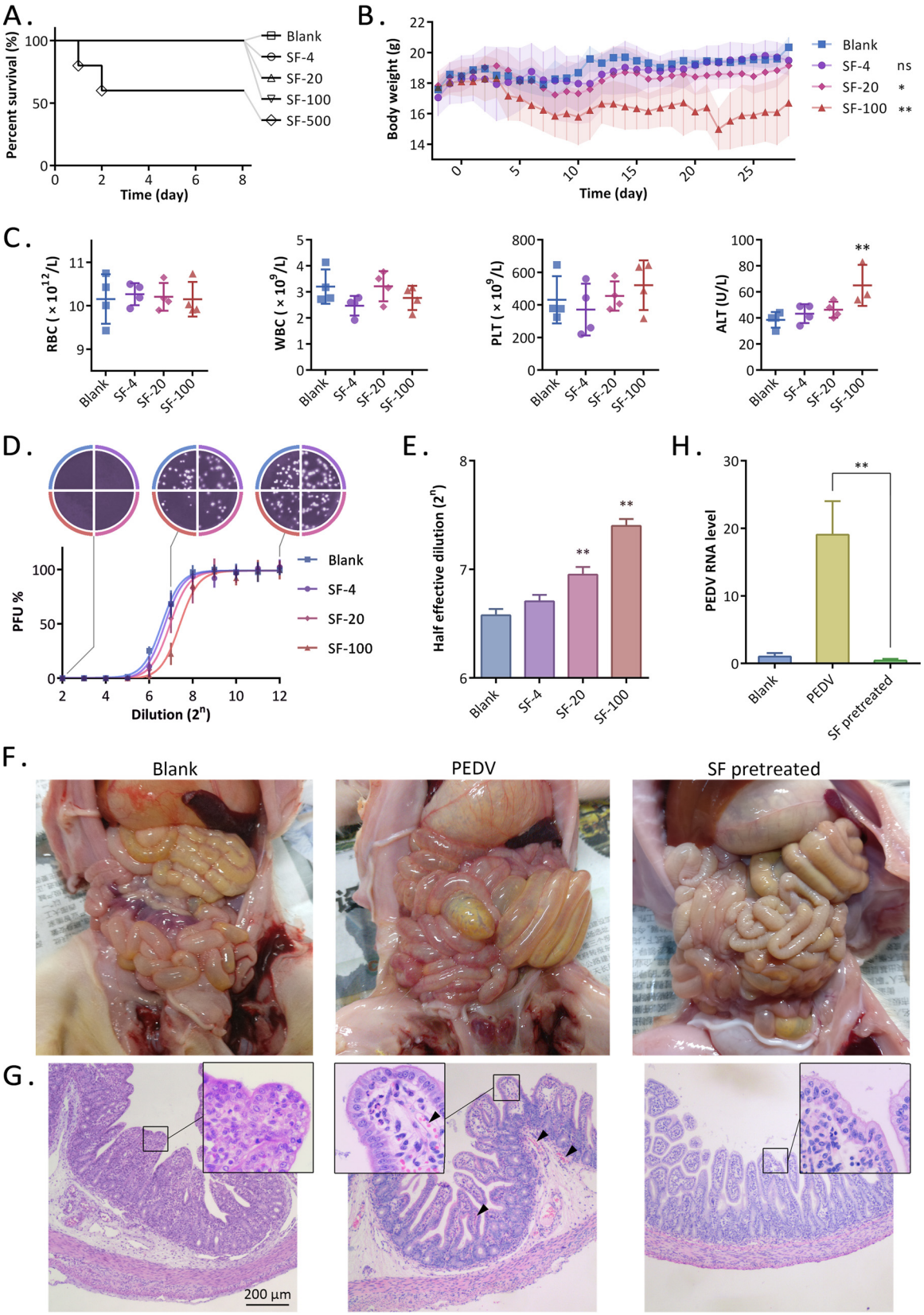

FIG 8 Oral administration of surfactin can protect against PEDV infection. (A) Survival curves of mice. The mice were orally administered surfactin in a single dose of 0, 4, 20, 100, or 500 mg/kg bw. (B to E) Subchronic toxicity evaluation of oral surfactin in mice. (B) The daily oral doses of surfactin for the 4 groups of mice were 0, 4, 20, and 100 mg/kg bw, respectively. Body weight was monitored and plotted. (C) Mice were sacrificed at day 28, and red blood cells (RBC), white blood cells (WBC), platelets (PLT), and alanine aminotransferase (ALT)

(Continued on next page)

anti-PEDV activity, and we confirm its anti-TGEV activity, in agreement with previous reports that surfactin exhibits activity against various enveloped viruses, such as herpes simplex virus 1 (HSV-1) and HSV-2, vesicular stomatitis virus, simian immunodeficiency virus, and Newcastle disease virus (21, 22). Previous investigations of the mechanism underlying the antiviral properties of surfactin have been inconclusive. Vollenbroich et al. reported that surfactin at 80 μM inactivates various enveloped viruses at room temperature (22°C), and membrane disruption by surfactin has been revealed by electron microscopy (21). Kracht et al. reported that 40 μM surfactin can disrupt the envelope of Semliki Forest virus (SFV) (31). However, the concentrations of envelope-destroying surfactin used in both cases exceed the levels at which cytotoxicity occurs. In the experiments described here, the concentration of surfactin used for our mechanistic studies was 20 μg/ml (about 20 μM), a level that neither causes hemolysis nor inhibits cell proliferation. At this cell-compatible concentration, surfactin does not disrupt the integrity of the viral envelope but rather inhibits the virus via a novel mechanism.

Experimental evidence and theoretical models indicate that the envelope-cell membrane fusion process involves the formation of a lipid stalk, accompanied by a positive-to-negative membrane curvature transition. During this stage, the membrane outer leaflets join together while the inner leaflets remain independent (Fig. 9D). The insertion of rigid amphiphilic fusion inhibitors (RAFIs) into the viral envelope reduces the curvature tension of the envelope and inhibits its fusion with the cell membrane, interrupting the viral life cycle and reducing the infectivity of several unrelated enveloped viruses (15). Structure-activity relationship studies suggest that amphipathic compounds have antiviral activity when the cross-sectional area of the hydrophobic tail is smaller than that of the hydrophilic head (26). Compounds with this structure are also referred to as wedge-like lipids (32). The insertion of wedge-like lipids into a lipid bilayer bends the membrane away from the polar heads, conferring a positive curvature.

We found that the natural compound surfactin acts directly on virus particles in $<$10 min. The compound does not damage the integrity of the virus membrane or cause cytotoxic effects at sufficiently low concentrations. Surfactin targets the lipid component of the virus, and its ability to insert into the envelope was demonstrated using a synthetic fluorescent surfactin derivative. We also found that surfactin inhibits the fusion of the virus and the cell membrane. Thermodynamic experiments show that surfactin increases the positive curvature of a lipid monolayer, in accord with the characteristics of a membrane fusion inhibitor. As illustrated in Fig. 1A and 9A, surfactin has two carboxyl groups in the amino acid side chains of its heptapeptide loop, forming a bulky hydrophilic head, while the shorter hydrophobic side chains of the other amino acid residues reside in a single long fatty acid chain (24). Surfactin therefore forms an inverted-cone structure in a water-oil interface. When surfactin is inserted into a lipid monolayer, it would be expected to force adjacent lipid molecules to tilt away, creating a positive curvature (Fig. 9B). Similarly, the insertion of surfactin increases the positive curvature of the outer leaflet of the envelope (Fig. 9C). Increased positive curvature is not conducive to the formation of the lipid stalk, and thus, surfactin inhibits membrane fusion (Fig. 9D).

Surfactin may be the most promising membrane fusion inhibitor identified thus far. LPC, a wedge lipid membrane fusion inhibitor discovered in the 1990s (33, 34), has limited potential for drug development because it can be rapidly metabolized to glycerol phosphates or phospholipids by all living cells. RAFIs, represented by dUY11,

FIG 8 Legend (Continued)
were detected. (D) Mouse jejunal contents were serially diluted and were tested for anti-PEDV activity. The results were subjected to an S curve fit. (E) The calculated half-effective dilution was plotted. (F to H) Two-day-old piglets were challenged with PEDV or remained unchallenged (blank). SF group piglets were given surfactin orally every 6 h, starting 1 day before the challenge, at a dose of 20 mg/kg bw/day. Piglets in the PEDV group died within 48 h after challenge, and all other piglets were sacrificed 48 h after challenge. (F) Anatomical photos of the abdominal cavities of the piglets. (G) Histopathology of the piglet jejuna, stained by hematoxylin and eosin. Arrowheads indicate congestion. (H) Detection of levels of PEDV RNA in the jejuna of piglets by qRT-PCR.

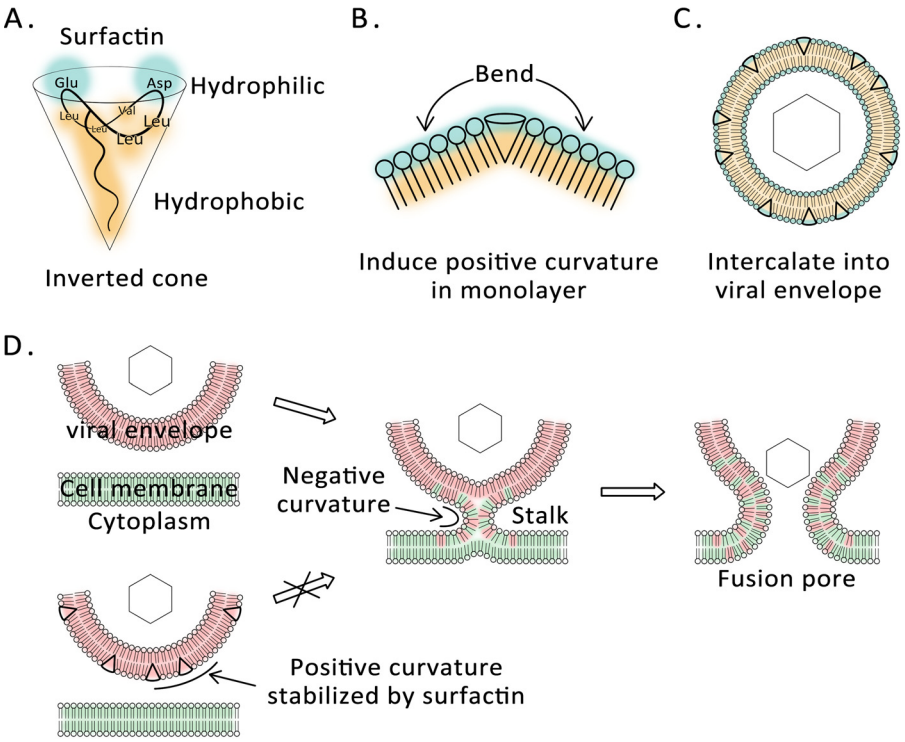

FIG 9 Model summarizing the mechanism underlying surfactin antiviral activity. (A) The surfactin molecule is a covalent ring consisting of a heptapeptide and a β-hydroxy lipid acid. The carboxyl groups of the two amino acid side chains form a hydrophilic head, and the remaining hydrophobic amino acids form a hydrophobic tail with the aliphatic chain. (B) Surfactin insertion bends a lipid monolayer toward its hydrophobic side. (C) Surfactin inserts into the outer leaflet of the viral envelope. (D) Surfactin insertion increases or stabilizes the positive curvature of the outer membrane leaflet. As a result, formation of the negatively curved membrane fusion intermediate is energetically less favorable.

were identified as wedge lipid membrane fusion inhibitors in earlier studies (26). Subsequent investigation revealed that the antiviral activity of dUY11 is abolished in the absence of light or can be reversed by singlet oxygen scavengers, suggesting that dUY11 is best described as a type II membrane-targeting photosensitizer (18). On the other hand, we found that oral administration of surfactin can protect piglets from PEDV challenge. Nontoxic oral doses can be as high as 20 mg/kg bw, which means that the concentration of the solution used is 500 times higher than the hemolytic concentration *in vitro*. This is consistent with reports that animals administered oral surfactin (35), mixed lipopeptides containing surfactin (36), or other lipopeptides (37) show higher tolerance than cells in *in vitro* experiments.

In summary, we have characterized a natural wedge lipid membrane fusion inhibitor, surfactin. Low concentrations of surfactin can be inserted into the viral envelope, stabilizing the positive curvature of the outer leaflet. This modification inhibits viral membrane fusion and is responsible for the antiviral activity of surfactin. Surfactin has potential as an antiviral drug, but its antiviral spectrum needs to be explored and verified. Antiviral effects on the enveloped viruses PEDV and TGEV have been demonstrated in our laboratory. Because surfactin targets the lipid component of the viral envelope, which is completely derived from the host cell (38), the emergence of surfactin-resistant viruses is unlikely. The present evidence indicates that surfactin has potential against enveloped viruses in the digestive tract. Further systematic usage requires higher cell compatibility. Other compounds with similar chemical structures may have superior characteristics. The lipopeptide family, represented by surfactin, offers a vast array of possibilities for finding optimal membrane fusion inhibitors and developing novel antiviral drugs. Alternatively, the structure of surfactin may be

modified chemically or by genetic engineering (39) in order to reduce toxicity and enhance the membrane fusion inhibition property.

MATERIALS AND METHODS

Reagents. Surfactin was extracted from the medium of a *B. subtilis* culture (strain OKB105) by following published methods (40). The purity of the product was 87%, as determined by LC-MS in comparison with commercially available surfactin (Sigma-Aldrich, St. Louis, MO). Dielaidoylphosphatidylethanolamine was obtained from Avanti Polar Lipids (Alabaster, AL, USA). Lysophosphatidylcholine was purchased from Sigma-Aldrich. SysLP1 and SysLP2 were synthesized by Synpeptide Co., Ltd. (Shanghai, China), with purity exceeding 95% as determined by HPLC.

Cells and viruses. Swine testicular (ST) cells (ATCC CRL-1746) were cultured in minimal essential medium (MEM) (Gibco, USA) supplemented with 10% fetal bovine serum (FBS; Gibco, USA). *Cercopithecus aethiops* kidney epithelial cells (Vero cells; ATCC CCL-81) and porcine intestinal columnar epithelial cells (IPEC-J2; DSMZ no. ACC-701; DSMZ, Germany) were cultured in Dulbecco's modified Eagle medium (DMEM) with high glucose (Gibco, USA), supplemented with 10% FBS (Gibco). All cells were cultured at 37°C under a humidified 5% CO_2 atmosphere. Cells were routinely seeded at a density of 2×10^5/ml in plastic tissue culture flasks (25-cm^2 flasks; Corning, USA) and were passaged every 3 to 4 days. PEDV (CV777) and TGEV (SHXB) were provided by the Jiangsu Provincial Academy of Environmental Science (JAAS) and were propagated in Vero and ST cells.

Detection of surfactin. Samples were analyzed by LC-MS (G2-XS QTof mass spectrometer; Waters). A 2-μl sample was injected into the ultraperformance LC (UPLC) column (2.1- by 100-mm Acquity UPLC BEH C_{18} column containing 1.7-μm particles) with a flow rate of 0.4 ml/min. Buffer A consisted of 0.1% formic acid in water, and buffer B consisted of 0.1% formic acid in acetonitrile. The gradient was 5% buffer B for 2 min, 5 to 95% buffer B for 15 min, and 95% buffer B for 2 min. Mass spectrometry was performed using an electrospray source in positive-ion mode, with a selected mass range of 50 to 1,200 *m/z*. The lock mass option was enabled using leucine-enkephalin (*m/z* 556.2771) for recalibration. The ionization parameters were as follows: capillary voltage, 2.5 kV; collision energy, 40 eV; source temperature, 120°C; desolvation gas temperature, 400°C. Data acquisition and processing were performed using MassLynx, version 4.1.

Detection of cytotoxicity. Hemolytic activity was measured using methods described by Deng et al. (41) with some modifications. Briefly, serial dilutions of surfactin were added to 200 μl of diluted mouse RBC (1%) in PBS, followed by incubation at 37°C for 1 h and centrifugation at $1,000 \times g$ for 10 min. A 100-μl volume of the supernatant was transferred to a well in a 96-well plate. The microplate reader (Infinite 200 PRO; Tecan Group Ltd., Switzerland) was used to measure the optical density at 540 nm (OD_{540}). Hemolysis (expressed as a percentage) was calculated as $(OD_S - OD_B)/(OD_P - OD_B) \times 100\%$, where OD_S, OD_B, and OD_P represent the optical densities of the surfactin-treated sample, the blank control, and the positive control, respectively. The positive control included 1% Triton X-100. All tests were run in triplicate.

The 3-(4,5-dimethyl-2-thiazolyl)-2,5-diphenyl-2H-tetrazolium bromide (MTT) assay was carried out according to the kit instructions. Briefly, IPEC-J2 or Vero cells grown in 96-well culture plates were incubated with a range of surfactin concentrations for 12 h at 37°C. The cells were then incubated for an additional 2 h with 0.8 mg/ml MTT dissolved in serum-free DMEM, and absorbance was recorded at 560 nm using a microplate spectrophotometer system (SpectraMax 190; Molecular Devices). Results were analyzed using SoftMax Pro (version 2.2.1) and are presented as percentages of the control values.

RNA extraction and RT-PCR. Total RNA was extracted from cells using TRIzol reagent (Invitrogen) according to the manufacturer's instructions. cDNA was generated by reverse transcription using HiScript QRT SuperMix for qPCR (Vazyme) according to the manufacturer's instructions. Nucleic acids of PEDV or TGEV were assayed by amplifying viral nucleoprotein (N) gene sequences using qRT-PCR with the TaKaRa SYBR green qPCR kit. Primer sequences were as follows: PEDV-N-F (sense), 5′-AAGGCGCAAAGACTGAA CCC-3′; PEDV-N-R (antisense), 5′-TGTTGCCATTACCACGACTCC-3′; TGEV-N-F (sense), 5′-CAATTCCCGTGGT CGGAAGA-3′; TGEV-N-R (antisense), 5′-TTTACGTTGGCCCTTCACCA-3′; S-scrofa-GAPDH-F, 5′-TCATCATCTC TGCCCCTTCT-3′; S-scrofa-GAPDH-R, 5′-GTCATGAGTCCCTCCACGAT-3′. Amplified products were quantitated using the comparative threshold cycle (C_T) method, and results were normalized to the endogenous levels of glyceraldehyde-3-phosphate dehydrogenase (GAPDH).

Time-of-addition assay. Confluent ST cells in 12-well plates were infected with 1,000 PFU of TGEV and were incubated for 1 h at 4°C to synchronize infection. The inoculum was removed; 1 ml of DMEM was added to each well; and samples were placed in a humidified incubator at 37°C. At various time points, a surfactin solution was added dropwise to the wells or to the virus samples, to a final concentration of 20 μg/ml. After 12 h, the supernatant was collected and was serially diluted, and the virus concentration was determined by a plaque assay. Viral nucleic acid and protein levels in the cells were measured by qRT-PCR and Western blotting. The data shown in the figures are representative of 3 independent experiments.

Plaque reduction assay. ST cells were seeded at 2×10^5/well in 24-well tissue culture plates and were incubated for 18 to 24 h at 37°C until approximately 95% confluent. TGEV (100 PFU) was mixed with an equal volume of surfactin in dimethyl sulfoxide (DMSO), or DMSO alone was mixed with surfactin, and the mixture was incubated at 37°C for 10 min, or as otherwise specified. The samples were added to the cells, and the cultures were incubated for 30 min at 4°C for to allow for virus adsorption. Cell supernatants were then removed; the cells were washed to remove any unattached virus; and DMEM with 1% agar was added to each well. After 48 h at 37°C, the cells were fixed with 4% formaldehyde, the agar overlays removed, and the cells stained with 0.1% crystal violet. The plaques in each well were

counted. Data are represented as the means ± standard deviations of results from 3 independent experiments. Curve fitting and medium effective concentrations (EC_{50}) were calculated with GraphPad Prism, version 6, using the log(inhibitor)-versus-response equation.

Lipid extraction and analysis. After the removal of excess surfactin in virus samples by gel filtration at a low temperature, the eluent (containing virus) was concentrated by low-pressure rotary evaporation. Viral lipids were extracted by the addition of chloroform-methanol (2:1, vol/vol), followed by 5% (vol/vol) freshly prepared saturated (28%, wt/wt) ammonia, using a previously published procedure (42). The lipid extract was concentrated by low-pressure rotary evaporation, and the surfactin component was quantitated by mass spectrometry.

Fluorescence detection. Dual-wavelength fluorescence scans were obtained using a Hitachi F-7000 fluorescence spectrophotometer (Hitachi Inc., Japan). Samples were labeled with 20 μg/ml synthetic lipopeptides. The final concentration of TGEV was 500 μg/ml for viral protein. The scanning field was set for emission spectra from 200 nm to 600 nm and for excitation spectra from 200 nm to 600 nm. Data collection and analysis were performed with FL Solutions, version 2.1, for the F-7000 spectrophotometer (Hitachi Inc., Japan).

Detection of envelope membrane integrity. Envelope membrane integrity was assessed as reported previously (43), with some modifications. Briefly, purified TGEV was treated with 20 μM surfactin, LPC, 0.01% Triton X-100, or a solvent (PBS) for 30 min at 37°C and was then sedimented through a linear 20%-to-50% (wt/vol) sucrose density gradient (10,000 × *g*, 2 h). Each gradient was sampled as 26 fractions, collected using a capillary siphon. The mass of a 200-μl sample from each fraction was accurately measured at room temperature in order to calculate density. The percentage of sucrose was determined using the following formula (44): $\text{pct} = -142.84\rho^2 + 534.52\rho - 390.71$, where pct is the percentage of sucrose and ρ is the density of the sample. A sample from each fraction was subjected to SDS-PAGE and was then probed on a Western blot to detect spike protein and nucleoprotein. A second sample from each fraction was used for viral nucleic acid detection, and a third sample was used to conduct a plaque assay to determine the titers of infectious particles (PFU).

Membrane fusion assay. Octadecyl rhodamine (R18)-labeled enveloped virus can be directly fused to the plasma membrane at a low pH (<6), and fusion can be detected by fluorescence due to R18 dequenching (45). R18-labeled TGEV fusion experiments were performed as described previously (15, 26), with modifications. The fluorescent probe was inserted into the viral bilayer by the addition of 15 μl of a 1.4 mM R18 (Sigma-Aldrich, St. Louis, MO) solution in ethanol, with vigorous vortexing, to 1 ml of NaCl-HEPES containing 1 mg of virus protein. After incubation for 1 h at 37°C, unbound probe was removed with fluorescent dye removal columns (Thermo Fisher Scientific, USA). R18-labeled-TGEV was exposed to surfactin, LPC, DEPE, or a solvent (PBS) for 10 min at 37°C. Virus samples were added to monolayers of ST cells in a 96-well plate and were incubated for 1 h at 4°C. Cell supernatants were then removed, and the cells were washed with fusion buffer (10 mM HEPES, 10 mM morpholineethanesulfonic acid [MES], 140 mM NaCl [pH 7.4]) at 4°C. Fusion buffer at pH 5 was added to each well, and the fluorescence intensity was continuously monitored at 37°C for 1 h. Fluorescence was excited at 560 nm and detected at 590 nm using a microplate reader (Infinite 200 PRO; Tecan, Switzerland). The percentage of fusion was calculated as $(F_x - F_{\text{initial}})/(F_{\text{max}} - F_{\text{initial}})$, where F_x is the fluorescence at each time point, F_{initial} is the initial fluorescence of the sample, and F_{max} is the fluorescence resulting from the addition of Triton X-100 to a final concentration of 0.1% after the kinetic experiment.

Membrane curvature assay. The curvature tendency of a specific lipid compound in the lipid bilayer can be determined by differential scanning calorimetry (15). After DEPE (Avanti Polar Lipids, Alabaster, AL) was mixed with a small amount of surfactin, LPC, or cholesterol in chloroform-methanol (2:1), samples were dried under nitrogen gas and were placed in a vacuum desiccator for 3 h. The dried films were hydrated with 0.8 ml of 20 mM piperazine-*N*,*N*′-bis(2-ethanesulfonic acid) (PIPES), 0.14 M NaCl, 1 mM EDTA (pH 7.4) by vortexing, degassed, and placed in the calorimeter cell (DSC1; Mettler-Toledo AG). The lamellar-to-inverted-hexagonal phase transition temperature was evaluated at a heating scan rate of 1°C/min. The results were analyzed using STAR^e.

Animal experiments. The animal studies were approved by the Institutional Animal Care and Use Committee of Nanjing Agricultural University and followed National Institutes of Health guidelines for the performance of animal experiments. For the subchronic toxicity assessment, 40 mice (BALB/c) were divided into 4 groups. Each mouse either was left untreated or was intragastrically administered 0.1 ml of a surfactin solution at a dose of 4, 20, or 100 mg/kg bw, and the body weight was measured. The experiment lasted for 28 days; then the mice were sacrificed, and samples were collected. Blood samples from the same group were combined, and blood cell detection and blood biochemical tests were performed. The contents of the jejuna of the mice were centrifuged (12,000 × *g*, 5 min), heated (98°C, 10 min), and centrifuged again (12,000 × *g*, 5 min), and the supernatant was collected. The PEDV plaque reduction test was performed after serial dilution. For the PEDV protection experiment, 9 newborn piglets were divided into three groups, kept in incubators, and manually fed 10 ml milk every 3 h. From 24 h postbirth, the surfactin treatment group received 2 ml of a surfactin solution every 6 h before feeding, at a dose of 20 mg/kg bw. Other piglets were orally administered the same amount of PBS at the same time. At 48 h postbirth, piglets of the PEDV group and the surfactin treatment group were challenged by PEDV after feeding. Piglets that died in the PEDV group were immediately necropsied and sampled. The other piglets were sacrificed 48 h after infection, and samples were collected. The jejunal tissues of piglets were examined by histopathology and qRT-PCR for the PEDV genome.

ACKNOWLEDGMENTS

This work was supported by grant 31772777 from the National Natural Science Foundation of China and funded by the Priority Academic Program Development of Jiangsu Higher Education Institutions (PAPD).

REFERENCES

1. Buchmann JP, Holmes EC. 2015. Cell walls and the convergent evolution of the viral envelope. Microbiol Mol Biol Rev 79:403–418. https://doi.org/10.1128/MMBR.00017-15.
2. Weber DS, Alroy KA, Scheiner SM. 2017. Phylogenetic insight into Zika and emerging viruses for a perspective on potential hosts. Ecohealth 14:214–218. https://doi.org/10.1007/s10393-017-1237-x.
3. Sun RQ, Cai RJ, Chen YQ, Liang PS, Chen DK, Song CX. 2012. Outbreak of porcine epidemic diarrhea in suckling piglets, China. Emerg Infect Dis 18:161–163. https://doi.org/10.3201/eid1801.111259.
4. Gu JP, Yue XW, Xing R, Li CY, Yang ZB. 2012. Progress in genetically engineered vaccines for porcine transmissible gastroenteritis virus. Rev Med Vet (Toulouse) 163:107–111.
5. Lee C. 2015. Porcine epidemic diarrhea virus: an emerging and re-emerging epizootic swine virus. Virol J 12:193. https://doi.org/10.1186/s12985-015-0421-2.
6. Boniotti MB, Papetti A, Lavazza A, Alborali G, Sozzi E, Chiapponi C, Faccini S, Bonilauri P, Cordioli P, Marthaler D. 2016. Porcine epidemic diarrhea virus and discovery of a recombinant swine enteric coronavirus, Italy. Emerg Infect Dis 22:83–87. https://doi.org/10.3201/eid2201.150544.
7. Pearce SC, Schweer WP, Schwartz KJ, Yoon KJ, Lonergan SM, Gabler NK. 2016. Pig jejunum protein profile changes in response to a porcine epidemic diarrhea virus challenge. J Anim Sci 94(Suppl 3):412–415. https://doi.org/10.2527/jas.2015-9815.
8. Hanke D, Jenckel M, Petrov A, Ritzmann M, Stadler J, Akimkin V, Blome S, Pohlmann A, Schirrmeier H, Beer M, Hoper D. 2015. Comparison of porcine epidemic diarrhea viruses from Germany and the United States, 2014. Emerg Infect Dis 21:493–496. https://doi.org/10.3201/eid2103.141165.
9. Teissier E, Penin F, Pecheur EI. 2010. Targeting cell entry of enveloped viruses as an antiviral strategy. Molecules 16:221–250. https://doi.org/10.3390/molecules16010221.
10. White JM, Whittaker GR. 2016. Fusion of enveloped viruses in endosomes. Traffic 17:593–614. https://doi.org/10.1111/tra.12389.
11. Stachowiak JC, Brodsky FM, Miller EA. 2013. A cost-benefit analysis of the physical mechanisms of membrane curvature. Nat Cell Biol 15:1019–1027. https://doi.org/10.1038/ncb2832.
12. Melikyan GB. 2010. Driving a wedge between viral lipids blocks infection. Proc Natl Acad Sci U S A 107:17069–17070. https://doi.org/10.1073/pnas.1012748107.
13. Kielian M. 2014. Mechanisms of virus membrane fusion proteins. Annu Rev Virol 1:171–189. https://doi.org/10.1146/annurev-virology-031413-085521.
14. Wei X, Decker JM, Liu H, Zhang Z, Arani RB, Kilby JM, Saag MS, Wu X, Shaw GM, Kappes JC. 2002. Emergence of resistant human immunodeficiency virus type 1 in patients receiving fusion inhibitor (T-20) monotherapy. Antimicrob Agents Chemother 46:1896–1905. https://doi.org/10.1128/AAC.46.6.1896-1905.2002.
15. Colpitts CC, Ustinov AV, Epand RF, Epand RM, Korshun VA, Schang LM. 2013. 5-(Perylen-3-yl)ethynyl-arabino-uridine (aUY11), an arabino-based rigid amphipathic fusion inhibitor, targets virion envelope lipids to inhibit fusion of influenza virus, hepatitis C virus, and other enveloped viruses. J Virol 87:3640–3654. https://doi.org/10.1128/JVI.02882-12.
16. Hollmann A, Castanho MA, Lee B, Santos NC. 2014. Singlet oxygen effects on lipid membranes: implications for the mechanism of action of broad-spectrum viral fusion inhibitors. Biochem J 459:161–170. https://doi.org/10.1042/BJ20131058.
17. McGuigan C, Wang Y, Riley PA. 1994. Synthesis and biological evaluation of phosphate triester alkyl lysophospholipids (ALPs) as novel potential anti-neoplastic agents. Anticancer Drug Des 9:539–548.
18. Vigant F, Hollmann A, Lee J, Santos NC, Jung ME, Lee B. 2014. The rigid amphipathic fusion inhibitor dUY11 acts through photosensitization of viruses. J Virol 88:1849–1853. https://doi.org/10.1128/JVI.02907-13.
19. Wu YS, Ngai SC, Goh BH, Chan KG, Lee LH, Chuah LH. 2017. Anticancer activities of surfactin and potential application of nanotechnology assisted surfactin delivery. Front Pharmacol 8:761. https://doi.org/10.3389/fphar.2017.00761.
20. Kowall M, Vater J, Kluge B, Stein T, Franke P, Ziessow D. 1998. Separation and characterization of surfactin isoforms produced by Bacillus subtilis OKB 105. J Colloid Interface Sci 204:1–8. https://doi.org/10.1006/jcis.1998.5558.
21. Vollenbroich D, Ozel M, Vater J, Kamp RM, Pauli G. 1997. Mechanism of inactivation of enveloped viruses by the biosurfactant surfactin from Bacillus subtilis. Biologicals 25:289–297. https://doi.org/10.1006/biol.1997.0099.
22. Huang X, Lu Z, Zhao H, Bie X, Lü F, Yang S. 2006. Antiviral activity of antimicrobial lipopeptide from Bacillus subtilis fmbj against pseudorabies virus, porcine parvovirus, Newcastle disease virus and infectious bursal disease virus in vitro. Int J Peptide Res Ther 12:373–377. https://doi.org/10.1007/s10989-006-9041-4.
23. Wang X, Hu W, Zhu L, Yang Q. 2017. Bacillus subtilis and surfactin inhibit the transmissible gastroenteritis virus from entering the intestinal epithelial cells. Biosci Rep 37:BSR20170082. https://doi.org/10.1042/BSR20170082.
24. Tsan P, Volpon L, Besson F, Lancelin JM. 2007. Structure and dynamics of surfactin studied by NMR in micellar media. J Am Chem Soc 129:1968–1977. https://doi.org/10.1021/ja066117q.
25. Polozov IV, Bezrukov L, Gawrisch K, Zimmerberg J. 2008. Progressive ordering with decreasing temperature of the phospholipids of influenza virus. Nat Chem Biol 4:248–255. https://doi.org/10.1038/nchembio.77.
26. St Vincent MR, Colpitts CC, Ustinov AV, Muqadas M, Joyce MA, Barsby NL, Epand RF, Epand RM, Khramyshev SA, Valueva OA, Korshun VA, Tyrrell DL, Schang LM. 2010. Rigid amphipathic fusion inhibitors, small molecule antiviral compounds against enveloped viruses. Proc Natl Acad Sci U S A 107:17339–17344. https://doi.org/10.1073/pnas.1010026107.
27. Yeagle PL, Smith FT, Young JE, Flanagan TD. 1994. Inhibition of membrane fusion by lysophosphatidylcholine. Biochemistry 33:1820–1827. https://doi.org/10.1021/bi00173a027.
28. Sample CJ, Hudak KE, Barefoot BE, Koci MD, Wanyonyi MS, Abraham S, Staats HF, Ramsburg EA. 2013. A mastoparan-derived peptide has broad-spectrum antiviral activity against enveloped viruses. Peptides 48:96–105. https://doi.org/10.1016/j.peptides.2013.07.014.
29. Takahashi H, Sinoda K, Hatta I. 1996. Effects of cholesterol on the lamellar and the inverted hexagonal phases of dielaidoylphosphatidylethanolamine. Biochim Biophys Acta 1289:209–216. https://doi.org/10.1016/0304-4165(95)00170-0.
30. Nielsen DS, Shepherd NE, Xu W, Lucke AJ, Stoermer MJ, Fairlie DP. 2017. Orally absorbed cyclic peptides. Chem Rev 117:8094–8128. https://doi.org/10.1021/acs.chemrev.6b00838.
31. Kracht M, Rokos H, Ozel M, Kowall M, Pauli G, Vater J. 1999. Antiviral and hemolytic activities of surfactin isoforms and their methyl ester derivatives. J Antibiot 52:613–619. https://doi.org/10.7164/antibiotics.52.613.
32. Vigant F, Santos NC, Lee B. 2015. Broad-spectrum antivirals against viral fusion. Nat Rev Microbiol 13:426–437. https://doi.org/10.1038/nrmicro3475.
33. Günther-Ausborn S, Stegmann T. 1997. How lysophosphatidylcholine inhibits cell-cell fusion mediated by the envelope glycoprotein of human immunodeficiency virus. Virology 235:201–208. https://doi.org/10.1006/viro.1997.8699.
34. Vogel SS, Leikina EA, Chernomordik LV. 1993. Lysophosphatidylcholine reversibly arrests exocytosis and viral fusion at a stage between triggering and membrane merger. J Biol Chem 268:25764–25768.
35. Hwang YH, Kim MS, Song IB, Park BK, Lim JH, Park SC, Yun HI. 2009. Subacute (28 day) toxicity of surfactin C, a lipopeptide produced by Bacillus subtilis, in rats. J Health Sci 55:351–355. https://doi.org/10.1248/jhs.55.351.
36. Ben Ayed H, Nasri R, Jemil N, Ben Amor I, Gargouri J, Hmidet N, Nasri M. 2015. Acute and sub-chronic oral toxicity profiles of lipopeptides from Bacillus mojavensis A21 and evaluation of their in vitro anticoagulant activity. Chem Biol Interact 236:1–6. https://doi.org/10.1016/j.cbi.2015.04.018.

37. Gu K, Zhang D, Guan C, Xu J, Li S, Shen G, Luo Y, Li Y. 2017. Safe antifungal lipopeptides derived from Bacillus marinus B-9987 against grey mold caused by Botrytis cinerea. J Integr Agric 16:1999–2008. https://doi.org/10.1016/S2095-3119(16)61616-7.
38. Kates M, Allison AC, Tyrrell DAJ, James AT. 1961. Lipids of influenza virus and their relation to those of the host cell. Biochim Biophys Acta 52:455–466. https://doi.org/10.1016/0006-3002(61)90403-6.
39. Dufour S, Deleu M, Nott K, Wathelet B, Thonart P, Paquot M. 2005. Hemolytic activity of new linear surfactin analogs in relation to their physico-chemical properties. Biochim Biophys Acta 1726:87–95. https://doi.org/10.1016/j.bbagen.2005.06.015.
40. Gao X, Yao S, Huong P, Joachim V, Wang J. 2003. Purification and identification of surfactin isoforms produced by Bacillus subtilis B2 strain. Wei Sheng Wu Xue Bao 43:647–652. (In Chinese.)
41. Deng JD, He B, He DH, Chen ZF. 2016. A potential biopreservative: chemical composition, antibacterial and hemolytic activities of leaves essential oil from Alpinia guinanensis. Ind Crops Prod 94:281–287. https://doi.org/10.1016/j.indcrop.2016.09.004.
42. Aloia RC, Tian HR, Jensen FC. 1993. Lipid-composition and fluidity of the human immunodeficiency virus envelope and host cell plasma membranes. Proc Natl Acad Sci U S A 90:5181–5185.
43. Wolf MC, Freiberg AN, Zhang TH, Akyol-Ataman Z, Grock A, Hong PW, Li JR, Watson NF, Fang AQ, Aguilar HC, Porotto M, Honko AN, Damoiseaux R, Miller JP, Woodson SE, Chantasirivisal S, Fontanes V, Negrete OA, Krogstad P, Dasgupta A, Moscona A, Hensley LE, Whelan SP, Faull KF, Holbrook MR, Jung ME, Lee B. 2010. A broad-spectrum antiviral targeting entry of enveloped viruses. Proc Natl Acad Sci U S A 107:3157–3162. https://doi.org/10.1073/pnas.0909587107.
44. Honig P. 1953. Principles of sugar technology, vol 1. Elsevier, Amsterdam, Netherlands.
45. Blumenthal R, Bali-Puri A, Walter A, Covell D, Eidelman O. 1987. pH-dependent fusion of vesicular stomatitis virus with Vero cells. Measurement by dequenching of octadecyl rhodamine fluorescence. J Biol Chem 262:13614–13619.
46. Yang H, Li X, Li X, Yu H, Shen Z. 2015. Identification of lipopeptide isoforms by MALDI-TOF-MS/MS based on the simultaneous purification of iturin, fengycin, and surfactin by RP-HPLC. Anal Bioanal Chem 407:2529–2542. https://doi.org/10.1007/s00216-015-8486-8.